Temperature dependence of infrared-absorption lines of Co^{2+} in cadmium halides

A. P. Vink,[1,2] A. Meijerink,[1] and G. D. Jones[3]
[1]*Department of Condensed Matter, Debye Institute, P.O. Box 80000, 3508 TA Utrecht, The Netherlands*
[2]*Interfaculty Reactor Institute, Delft University of Technology, Mekelweg 15, 2629 JB Delft, The Netherlands*
[3]*Department of Physics and Astronomy, University of Canterbury, P.O. Box 4800, Christchurch, 8020, New Zealand*
(Received 10 April 2002; revised manuscript received 13 June 2002; published 30 October 2002)

Temperature-dependent infrared-absorption measurements were performed on the spin orbit and trigonal-crystal-field split levels of the $^4T_{1g}$ cubic-field ground term of Co^{2+} ($3d^7$) in the cadmium halides CdX_2 (X: Cl, Br, and I). Besides $\gamma_4^+ \rightarrow \gamma_4^+$ and $\gamma_4^+ \rightarrow \gamma_{5,6}^+$ electronic transitions, sharp vibronic lines are observed. From temperature-dependent line shift and line-broadening measurements of these lines, electron-phonon coupling parameters were determined. For Co^{2+} in $CdCl_2$, where the energy separation of the γ_4^+ and $\gamma_{5,6}^+$ levels studied is comparable to the phonon energies, a contribution from direct one-phonon processes needs to be included. Further line-shift measurements were made on Co^{2+} pair lines to determine whether the electron-phonon coupling differed for Co^{2+} pairs, with no significant difference being observed. The infrared-absorption spectrum for Co^{2+} in CdI_2 is reported.

DOI: 10.1103/PhysRevB.66.134303 PACS number(s): 71.20.Be

I. INTRODUCTION

The electron-phonon coupling for intraband $4f^n$ transitions in lanthanide ions has been investigated by determining vibronic-transition probabilities[1,2] and by measuring temperature-dependent broadening of spectral lines.[2–4] Because of the shielding of the $4f$ electrons from the surrounding ligands by filled $5s$ and $5p$ outer shells, these electron-phonon coupling effects are weak. For the transition-metal ions, the $3d^n$ transitions are characterized by stronger electron-phonon coupling effects with two types of transitions distinguished. If the transition within the $3d^n$ configuration is between d orbitals with a different $t_{2g}^n e_g^m$ composition (for example, a t_{2g} (nonbonding)$\rightarrow$e$_g$ (antibonding) transition in octahedral symmetry) the transition appears as a broad band. If a transition within the $3d^n$ configuration does not involve a change in bonding (for example, a spin-flip transition within the same $t_{2g}^n e_g^m$ composition), a sharp line is observed. To study the electron-phonon coupling by measurements of temperature-dependent line broadening, sharp-line transitions are needed and the choice of $3d^n$ ions for this is rather limited. The only $3d^n$ ions for which electron-phonon effects have been studied in some detail are Cr^{3+} and V^{2+}, both of which show sharp-line emission from a spin-flip transition within the $3d^3$ configuration[5–7] in $Al_2O_3:Cr^{3+}/V^{2+}$ (Refs. 5 and 6) and $MgO:Cr^{3+}$.[7] It seemed that for line broadening the Raman two-phonon process was dominant. Kushida determined the contribution of the direct one-phonon processes to the line broadening in Ref. 6. The influence of covalency of the host lattice on the electron-phonon coupling[8,9] and differences in the electron-phonon coupling for single Cr^{3+} ions and Cr^{3+} ion pairs have already been reported.[10,11]

In this paper, the electron-phonon coupling is investigated for transitions between spin-orbit split components of the $^4T_{1g}$ ground cubic-field term of Co^{2+} ($3d^7$) in CdX_2 (X = Cl, Br, I). Because spin-orbit coupling is of the order of 700 cm^{-1} for Co^{2+}, these transitions occur as sharp lines in infrared-absorption spectra.

All three cadmium halides have a layered structure. Both $CdBr_2$ and $CdCl_2$ have a similar structure, with the D_{3d}^5 space group,[12,13] while CdI_2 is slightly different with a crystal structure with the C_{6v}^4 space group.[13,14] Both type of structures have the same sheets of linked CdX_6 octahedra, with different stacking of the layers for CdI_2.[13]

The electron-phonon coupling for these transitions of Co^{2+} in $CdCl_2$ and $CdBr_2$ is investigated by temperature-dependent line-broadening and line-shift measurements. For $CdBr_2:Co^{2+}$, the electron-phonon coupling for transitions of both single Co^{2+} ions and Co^{2+} pairs is examined. Infrared transitions observed for Co^{2+} in CdI_2 are reported and compared with those for Co^{2+} in $CdCl_2$ and $CdBr_2$.

II. THEORY

A. Infrared spectroscopy of Co^{2+} in cadmium halides

The spectroscopy of Co^{2+} is well established. The free-ion ground-state ^4F is split by an octahedral crystal field into a ground $^4T_{1g}$ term and $^4T_{2g}$ and $^4A_{2g}$ terms. Here the Mulliken notation is adopted, while levels resulting from splitting of these cubic-field terms by spin-orbit coupling and trigonal distortions are labeled in the Bethe γ notation.[17] The $^4T_{1g} \rightarrow {}^4T_{2g}$ transition between the two lowest cubic-crystal-field terms occurs in the near infrared[18] around 7 000 cm^{-1} as a broad band. The ground $^4T_{1g}$ term is split by spin-orbit coupling and the D_{3d}-symmetry trigonal crystal field into 6 Kramers-degenerate γ_4^+ and $\gamma_{5,6}^+$ levels, with the $\gamma_{5,6}^+$ levels two-fold degenerate in the absence of a magnetic field.[15] The resulting energy-level splitting pattern is given in Fig. 1. Infrared-absorption transitions from the γ_4^+ ground level to the γ_4^+ and $\gamma_{5,6}^+$ levels are all magnetic-dipole allowed.

In the infrared-absorption spectrum of Co^{2+} in $CdBr_2$, two single Co^{2+} electronic lines are observed; one at 887 cm^{-1} to a γ_4^+ level and the other at 893.1 cm^{-1} to a $\gamma_{5,6}^+$ level.[15] At higher Co^{2+} concentrations, additional absorption lines appear, which are attributed to transitions of Co^{2+} ion pairs.[15]

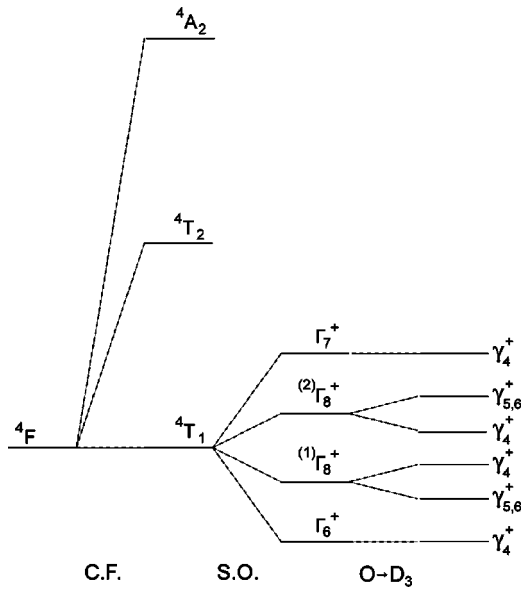

FIG. 1. Energy-level scheme showing the splitting of the ^{4}F multiplet by an octahedral crystal field and further splitting of the $^4T_{1g}$ ground term by spin-orbit coupling and a trigonal (D_{3d}) crystal field.

In the infrared-absorption spectrum of Co^{2+} in $CdCl_2$, three of these five magnetic-dipole allowed transitions have been observed. The lowest transition to the lower $\gamma_{5,6}^+$ level lies within the host-lattice absorption while the transition to the highest γ_4^+ level is obscured by a broad vibronic absorption band around 1 170 cm^{-1}. The three transitions observed have energies of 498.5 cm^{-1} (γ_4^+), 922.3 cm^{-1} (γ_4^+), and 951.1 cm^{-1} ($\gamma_{5,6}^+$) with the transition to the $\gamma_{5,6}^+$ level having the largest absorption.

B. Electron-phonon coupling effects

The electron-phonon coupling is the interaction between electronic states and lattice vibrations (phonons). The effect of the electron-phonon coupling on spectral lines is to increase spectral linewidths and to shift spectral-line positions with temperature.

The lifetime of an excited state is reduced at elevated temperatures by phonon-dephasing processes resulting in a larger uncertainty in the energy of a transition and broadening of the spectral line.[3] Besides the inhomogeneous linewidth E^{Inh}, there are several dephasing processes which contribute to the total homogeneous linewidth $E^{\mathrm{Hom}}(T)$:[3]

$$E(T)=E^{\mathrm{Inh}}+E^{\mathrm{Hom}}(T)=E^{\mathrm{Inh}}+E^{\mathrm{Orbach}}+E^{D}_{\mathrm{Abs}}+E^{D}_{\mathrm{Em}}+E^{\mathrm{Raman}}. \quad (1)$$

TABLE I. Positions (in cm^{-1}) of infrared-absorption lines for Co^{2+} in CdX_2 (X:Cl, Br, and I), vibronic-energy intervals (in cm^{-1}) for the sharp vibronic lines, lattice phonon cutoff frequencies (in cm^{-1}) and the Debye temperatures Θ_D (in K).

Transition		$CdCl_2$	$CdBr_2$	CdI_2
$\gamma_4^+\rightarrow\gamma_4^+$	electronic	922.7	887.7	
$\gamma_4^+\rightarrow\gamma_{5,6}^+$	electronic	952.1	893.5	850.5
$\gamma_4^+\rightarrow\gamma_4^+$	vibronic	995.8	947.4	897.0
$\gamma_4^+\rightarrow\gamma_{5,6}^+$	vibronic	1025.9	953.7	900.4
Vibronic interval	ΔE	73	60	50
Cutoff frequency	ω_{cutoff}	214	184	150
Debye temperature	Θ_D	310	260	215

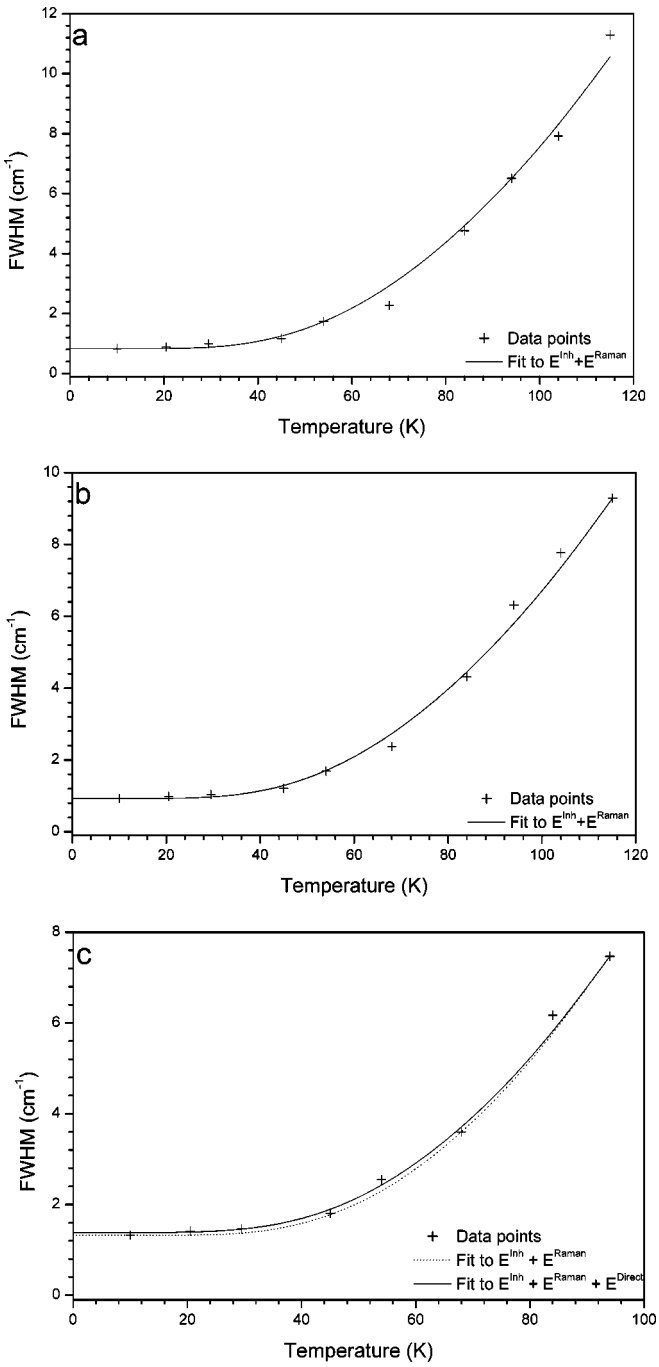

FIG. 2. Temperature dependence of the linewidth for various electronic and vibronic absorption lines corresponding to transitions on single Co^{2+} ions in $CdBr_2$:1%Co^{2+}. The different graphs represent the temperature-dependent line broadening for the $\gamma_4^+\rightarrow\gamma_{5,6}^+$ electronic line at 893.5 cm^{-1} (a), the $\gamma_4^+\rightarrow\gamma_4^+$ vibronic line at 947.4 cm^{-1} (b), and the $\gamma_4^+\rightarrow\gamma_{5,6}^+$ vibronic line at 953.7 cm^{-1} (c). The drawn lines are fits to Eq. (2).

TABLE II. Electron-phonon coupling parameters $\bar{\alpha}$ and β_{ij} for electronic and vibronic transitions determined for single Co^{2+} ions doped in $CdBr_2$ and $CdCl_2$ derived from a fit of the temperature-dependent linewidths to Eq. (2).

Host	Transition		E^{Inh}	$\bar{\alpha}$	β_{ij}	Process	Interval
	$\gamma_4^+ \rightarrow \gamma_{5,6}^+$	electronic	0.83	333	–	–	–
	$\gamma_4^+ \rightarrow \gamma_4^+$	vibronic	0.93	286	–	–	–
$CdBr_2$							
	$\gamma_4^+ \rightarrow \gamma_{5,6}^+$	vibronic	1.32	361	–	–	–
	$\gamma_4^+ \rightarrow \gamma_{5,6}^+$	vibronic	0.83	336	0.53	Emission	60
	$\gamma_4^+ \rightarrow \gamma_{5,6}^+$	electronic	1.95	260	0.96	Emission	30
					2.52	Absorption	73
$CdCl_2$	$\gamma_4^+ \rightarrow \gamma_4^+$	vibronic	1.95	134	0.42	Emission	73
					2.38	Absorption	30
	$\gamma_4^+ \rightarrow \gamma_{5,6}^+$	vibronic	1.95	1330	1.68	Emission	30

The inhomogeneous linewidth E^{Inh} is from strains and defects in the host crystal and is temperature independent.[3] The homogeneous linewidth $E^{\mathrm{Hom}}(T)$ is primarily determined by a Raman two-phonon dephasing process, giving a temperature-dependent contribution E^{Raman}.[3,5] The contribution of the Orbach two-phonon process E^{Orbach} is usually negligible. When electronic intervals have comparable energies to phonon energies, the direct processes E^D_{Abs} and E^D_{Em} of one-phonon absorption and emission also contribute to the line broadening. With both the Raman and the direct one-phonon processes included, the linewidth $E(T)$ as a function of temperature has the form[3,5,6]

$$E(T)=E^{\mathrm{Inh}}+\bar{\alpha}\left(\frac{T}{\Theta_D}\right)^7\int_0^{T/\Theta_D}\frac{x^6e^x}{(e^x-1)^2}dx$$

$$+\sum_{j<i}\beta_{ij}(n+1)+\sum_{j>i}\beta_{ij}n, \qquad (2)$$

where x is equal to $\hbar\omega/kT$ and the n is the Bose-Einstein phonon-occupation number $1/(e^{\hbar\omega/kT}-1)$.[3,5] The Debye temperature Θ_{D} is related the maximum phonon energy. In the Debye approximation, the phonon density of states increases as ω^2 up to the phonon cutoff energy ω_{cutoff}, with the Debye temperature defined by $k\Theta_{\mathrm{D}}=\hbar\omega_{\mathrm{cutoff}}$.

The electron-phonon parameters $\bar{\alpha}$ and β_{ij} may be determined by fitting the measured linewidths as a function of temperature, setting the low-temperature linewidth to the inhomogeneous linewidth E^{Inh} and adopting a value for the Debye temperature Θ_{D} derived from the vibrational spectrum of the host crystal.[3]

The line shift as a function of temperature also depends on the electron-phonon coupling.[5] Because of the decrease in crystal-field strength with temperature, the spectral lines usually shift to lower energy as a red shift. The line shift as a function of temperature can be fitted to the Raman two-phonon process by[5]

$$\epsilon(T)=\epsilon(0)+\epsilon^{\mathrm{Raman}}=\epsilon(0)+\alpha\int_0^{T/\Theta_D}\frac{x^3}{(e^x-1)}dx. \qquad (3)$$

Both x and Θ_{D} are as defined before, ϵ_0 is the position of the line at $T=0$ K and α is a further electron-phonon parameter.[5]

With the omission of any direct one-phonon contributions and adopting the same Debye temperature as used for the analyses of the line broadening, it is possible to determine the parameter α from a fit of the measured line shifts as a function of temperature.[5]

III. EXPERIMENTAL

A. Synthesis

Care has to be taken to prevent contamination by moisture of these hygroscopic-halide crystals $CdX_2:Co^{2+}$ (X=Cl, Br, I). The starting materials were first dried over several days under vacuum. To remove oxide or residual water, the starting materials of the appropriate cobalt and cadmium halide were heated to their melting point under a flow of of HBr or HCl in a furnace raised to 600 °C over a period of three hours. The molten liquid was passed through a quartz sieve into a tube, which was sealed off. The crystals were grown by the Bridgmann method of slowly lowering these sealed quartz ampoules through the temperature gradient of a furnace at 600 °C over three days.

For the $CdI_2:Co^{2+}$ crystals, the first purification step had to be omitted as HI gas decomposes at high temperatures. The starting materials were dried CdI_2 and CoI_2 powders, which were sealed off in glass ampoules. The crystals were grown by the Bridgman method at 425 °C.

B. Infrared-absorption measurements

0.25 cm^{-1} resolution infrared-absorption spectra were measured with a Bio-Rad FTS-40 Fourier transform infrared (FTIR) spectrometer over the 650–1400 cm^{-1} range which covers the transitions to the upper spin-orbit levels of Co^{2+} within the ground $^4T_{1g}$ cubic-field term. The crystal samples were mounted on a copper holder in thermal contact with the 10 K stage of a helium closed-cycle cryostat. Temperatures between 10 and 200 K were obtained by a temperature con-

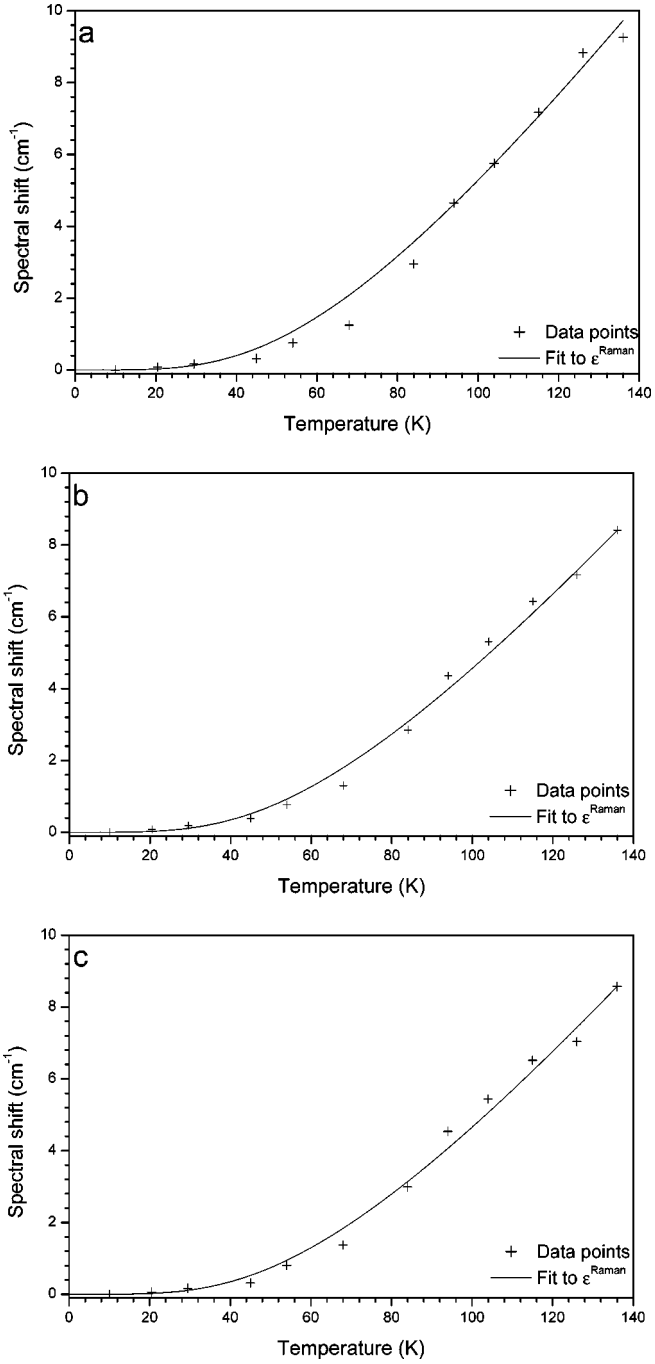

FIG. 3. Temperature-dependent line-shift measurements for transitions on single Co^{2+} ions in $CdBr_2$:1%Co^{2+}. In Fig. 3a the line shift for the $\gamma_4^+ \rightarrow \gamma_{5,6}^+$ electronic transition, whereas in Figs. 3b and 3c the shift for the vibronic $\gamma_4^+ \rightarrow \gamma_4^+$ and $\gamma_4^+ \rightarrow \gamma_{5,6}^+$ lines are shown. The drawn lines are fits to Eq. (3) using the Raman two-phonon process.

trol unit which regulated the current through an electric heater. The Win-IR curve-fit routine was used to determine spectral linewidths and shifts.

IV. RESULTS AND DISCUSSION

The infrared-absorption spectra for Co^{2+} ions in $CdCl_2$ and $CdBr_2$ have been reported[15,16] with both electronic and sharp vibronic lines being observed. We report temperature dependences of the widths and shifts of these electronic and sharp vibronic lines of Co^{2+}. Infrared-absorption spectra are reported also for single Co^{2+} ions in CdI_2. Table I summarizes the spectroscopic data, together with measured vibrational intervals for the sharp vibronic lines, the host-lattice phonon cutoff energies and adopted values for the Debye temperatures Θ_D. All these quantities show systematic trends along the chloride to iodide series, which are related to the increase in the ionic radius of the ligands from Cl^- to Br^- and I^-. As expected, the smallest ligand (Cl^-) gives the largest crystal-field splitting while its smaller mass gives higher lattice-vibration frequencies.

TABLE III. Electron-phonon coupling parameters α (in cm^{-1}) determined from absorption of 1 mole% of Co^{2+} in $CdBr_2$ and $CdCl_2$ measured from temperature-dependent line shifts.

Host	Transition		α
$CdBr_2$	$\gamma_4^+ \rightarrow \gamma_{5,6}^+$	electronic	122
	$\gamma_4^+ \rightarrow \gamma_4^+$	vibronic	105
	$\gamma_4^+ \rightarrow \gamma_{5,6}^+$	vibronic	107
$CdCl_2$	$\gamma_4^+ \rightarrow \gamma_4^+$	electronic	257
	$\gamma_4^+ \rightarrow \gamma_{5,6}^+$	electronic	147
	$\gamma_4^+ \rightarrow \gamma_4^+$	vibronic	182
	$\gamma_4^+ \rightarrow \gamma_{5,6}^+$	vibronic	190

The influence of ion-pairs on the electron-phonon coupling has been studied for $4f^n$ rare-earth ions and for $3d^n$ transition-metal ions. It had been reported that electron-phonon coupling was enhanced for lanthanide-ion pairs and theoretical models explaining the enhanced electron-phonon coupling strength were developed.[19–24] Later it turned out that the observation of enhanced intensity for vibronic lines in absorption spectra of lanthanides was related to saturation effects for the electronic lines at higher lanthanide concentrations and not to any specific concentration enhancement of the electron-phonon coupling.[25] For transition-metal ions, an influence of ion pairing may be apparent since the electron-phonon coupling is larger. To investigate this possibility, the

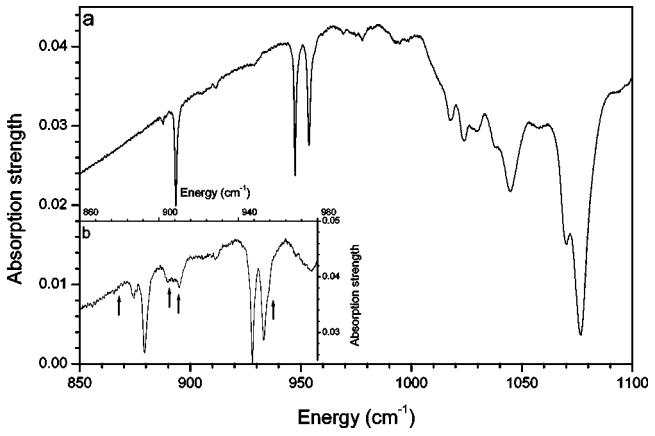

FIG. 4. 10 K infrared-absorption spectra of Co^{2+} in $CdBr_2$ for 1% Co^{2+} (a) and 5% Co^{2+} (inset b) concentrations. The absorption lines corresponding to Co^{2+} pairs are marked by arrows.

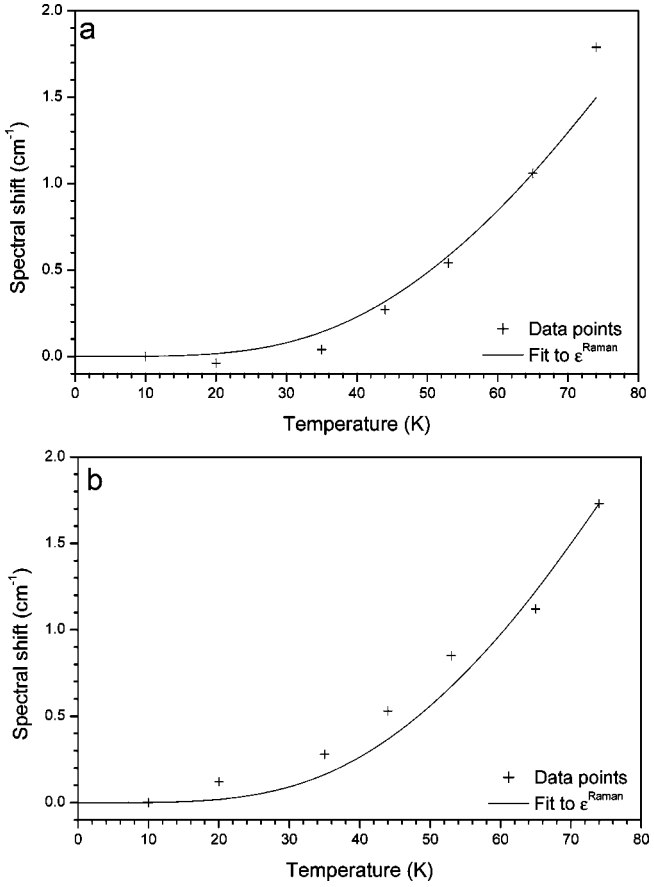

FIG. 5. Temperature-dependent line shifts for two Co^{2+} pair lines at 905 cm^{-1} (a) and 910 cm^{-1} (b) measured in $CdBr_2$:5% Co^{2+}. The drawn line is a fit to the line-shift given by the Raman process of Eq. (3).

shifts of Co^{2+} pair lines in $CdBr_2$ were also studied as a function of temperature.

The temperature-dependence results for each system are now discussed in turn.

A. $CdBr_2:Co^{2+}$

In Figs. 2(a), 2(b), and 2(c), the temperature-dependent line broadening of the $\gamma_4^+ \rightarrow \gamma_{5,6}^+$ electronic transition and the two $\gamma_4^+ \rightarrow \gamma_4^+$ vibronic and the $\gamma_4^+ \rightarrow \gamma_{5,6}^+$ vibronic lines are shown, while the $\gamma_4^+ \rightarrow \gamma_4^+$ electronic transition proved too weak to measure. The drawn lines in Fig. 2 represent fits to Eq. (2) with the resulting fit parameters summarized in Table II.

Figure 2 shows that the line broadening of all three transitions are all about the same. All the lines start to broaden above 40 K and rapidly increase in width between 40 and 100 K. Table II gives the values of around 300 cm^{-1} for the

TABLE IV. Electron-phonon coupling parameter α (in cm^{-1}) for single Co^{2+} ions and Co^{2+} ion pairs determined for $CdBr_2$:5% Co^{2+} crystals from temperature-dependent line-shift measurements.

Transition		Energy (cm^{-1})	α (cm^{-1})
$\gamma_4^+ \rightarrow \gamma_4^+$	electronic	887.4 cm^{-1}	108
$\gamma_4^+ \rightarrow \gamma_{5,6}^+$	electronic	892.8 cm^{-1}	101
$\gamma_4^+ \rightarrow \gamma_4^+$	vibronic	947.1 cm^{-1}	97
$\gamma_4^+ \rightarrow \gamma_{5,6}^+$	vibronic	952.8 cm^{-1}	100
Pair line	electronic	904.7 cm^{-1}	70
Pair line	electronic	910.5 cm^{-1}	81

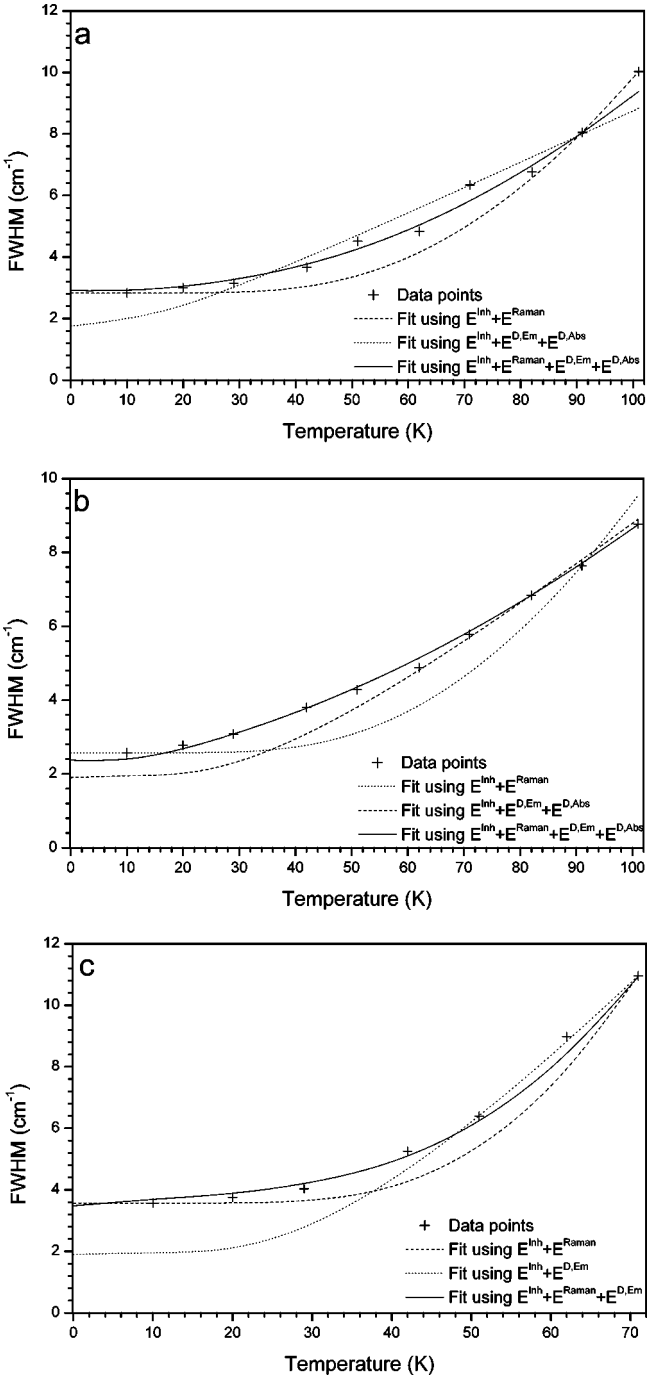

FIG. 6. Line-broadening for absorption lines of single Co^{2+} ions in $CdCl_2$:1%Co^{2+} showing the $\gamma_4^+ \rightarrow \gamma_{5,6}^+$ electronic transition (a), the $\gamma_4^+ \rightarrow \gamma_4^+$ vibronic transition (b) and the $\gamma_4^+ \rightarrow \gamma_{5,6}^+$ vibronic transition (c) with the fits to the Raman process both with and without contributions from direct one-phonon absorption and emission processes.

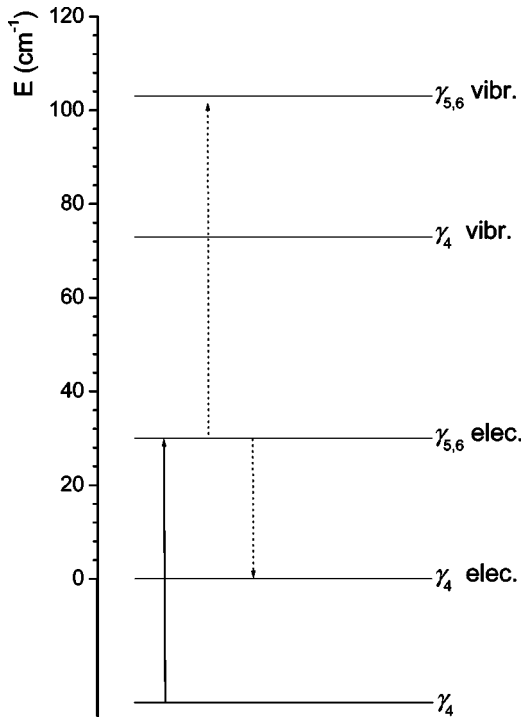

FIG. 7. Energy-level scheme of the Co^{2+} $\gamma_4^+ \rightarrow \gamma_{5,6}^+$ electronic transition in $CdCl_2$ showing the position of the electronic and vibronic levels relative to the γ_4^+ electronic level at 923 cm^{-1}. Both the electronic transition (solid line) and the two one-phonon transitions (broken line) are indicated.

electron-phonon parameter $\bar{\alpha}$ as derived from a fit of the data to Eq (2). Good fits are obtained with the Raman process alone and inclusion of contributions from direct one-phonon processes does not improve these fits.

For the line-broadening of the $\gamma_4^+ \rightarrow \gamma_{5,6}^+$ vibronic line, a fit including direct one-phonon emission was especially made. This was because this vibronic transition is a combination of an electronic transition to the $\gamma_{5,6}^+$ level coupled to a 60 cm^{-1} phonon and it was expected that emission of this 60 cm^{-1} phonon might contribute significantly to line broadening. Nevertheless, the result of this particular fit shows that any contribution from such 60 cm^{-1} phonon emission is negligible.

This result is confirmed by the measurements of the temperature-dependent line shifts as shown in Figs. 3(a), 3(b), and 3(c). The spectral positions as a function of temperature were fitted equally well with only the Raman two-phonon process. The derived α values from these fits are collected in Table III.

At higher Co^{2+} concentrations, Co^{2+} pair lines appear[15] and these lines were examined for $CdBr_2$. In Figs. 4(a) and 4(b), the infrared-absorption spectra of $CdBr_2$ with 1 mole % [4(a)] and with 5 mole % Co^{2+} [4(b), inset] are shown. For the higher-concentration crystal in the inset, a weak extra absorption line is observed at about 877 cm^{-1} (see arrow in the left in the inset), whose intensity increases at elevated temperatures. Additional features in this spectrum are a number of lines around 905 cm^{-1} and an absorption on the high-energy tail of the $\gamma_4 \rightarrow \gamma_{5,6}^+$ vibronic line (as indicated by other arrows in the inset).

At higher Co^{2+} concentrations, all absorption lines are broader through inhomogeneous broadening. As Co^{2+} pair lines occur close together, measuring their temperature-dependent linewidths was impracticable and only temperature-dependent line-shifts could be analyzed. These were carried out for the two Co^{2+} pair lines near 905 and 910 cm^{-1} shown in Fig. 5. Analysis of the shifts for both these pair lines for comparison with those for single Co^{2+} lines yielded the α values given in Table IV, which are all comparable. It has to be concluded that the electron-phonon coupling for single Co^{2+} and Co^{2+} ion pairs differ little. This is in agreement with the results found for Cr^{3+} ($3d^3$), where the electron-phonon coupling for Cr^{3+} pairs and single Cr^{3+} ions was found to be similar.[10,11]

B. $CdCl_2:Co^{2+}$

In Fig. 6 (a,b,c), the temperature-dependent broadening of the $\gamma_4^+ \rightarrow \gamma_{5,6}^+$ electronic line and the two $\gamma_4^+ \rightarrow \gamma_4^+$ and $\gamma_4^+ \rightarrow \gamma_{5,6}^+$ vibronic lines are shown. In contrast to the results for the line broadening of the corresponding transitions for Co^{2+} in $CdBr_2$, the Raman dephasing process alone could not account for the observed line broadening, especially over the temperature range from 40 to 70 K where the observed broadening is much more rapid than predicted by the Raman process.

To obtain a good fit, contributions from direct one-phonon processes need to be included between energy levels of Co^{2+} as shown in Fig. 7. As an example, for the $\gamma_4^+ \rightarrow \gamma_{5,6}^+$ electronic transition, two one-phonon processes contribute. One is emission of a 30 cm^{-1} phonon from the $\gamma_{5,6}^+$ electronic level at 952 cm^{-1} to the γ_4^+ electronic level at 922 cm^{-1} and the other is absorption of a 73 cm^{-1} phonon from the $\gamma_{5,6}^+$ vibronic level. The total linewidth for the $\gamma_4^+ \rightarrow \gamma_{5,6}^+$ electronic transition is then given by

$$E(T) = E^{Inh} + E^{\mathrm{Raman}} + E^{D}_{\mathrm{em\ 30\ cm^{-1}}} + E^{D}_{\mathrm{abs\ 73\ cm^{-1}}}. \qquad (4)$$

By including both these one-phonon contributions, good agreement with the observed line-broadening behavior is obtained. For other lines of Co^{2+} in $CdCl_2$ the temperature dependence of their linewidths was fitted including appropriate one-phonon processes as determined from the energy-level scheme of Fig. 7. The fits are shown in Fig. 6 and the corresponding fitting parameters listed in Table II. Inclusion of one-phonon processes results in a good agreement between the calculated and observed temperature dependences of the linewidths. However, for the $\gamma_4^+ \rightarrow \gamma_{5,6}^+$ vibronic transition, an anomalously large value of $\bar{\alpha}$ is found suggesting that further one-phonon emission and absorption processes may be involved.

The fit of the line-shifts of Co^{2+} in $CdCl_2$ using only α and Θ_D as fit parameters are shown in Fig. 8 with the parameter values listed in Table III. Here the agreement between the fits and the observed temperature dependence of the line shifts is poor, which indicates one-phonon processes are needed for interpretation of line shifts, as well as line broadening.

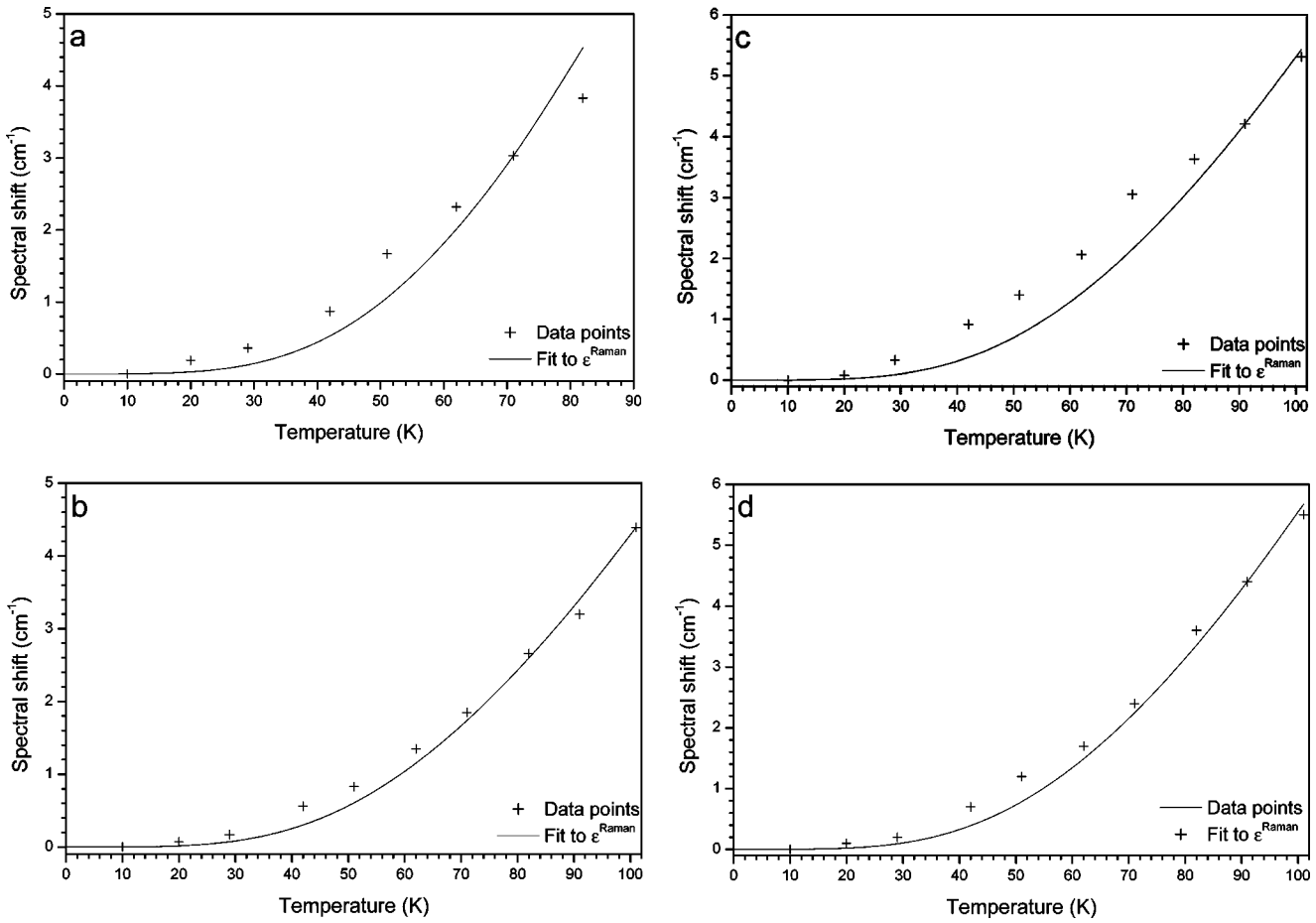

FIG. 8. Line-shifts measured for absorption lines of single Co^{2+} ions in $CdCl_2$:1%Co^{2+} showing the $\gamma_4^+ \rightarrow \gamma_4^+$ electronic transition (a), the $\gamma_4^+ \rightarrow \gamma_{5,6}^+$ electronic transition (b), the $\gamma_4^+ \rightarrow \gamma_4^+$ vibronic transition (c) and the $\gamma_4^+ \rightarrow \gamma_{5,6}^+$ vibronic transition (d) with their fit to the Raman process.

To understand why the direct one-phonon processes do have a significant contribution for Co^{2+} in $CdCl_2$ and not for Co^{2+} in $CdBr_2$, the difference in the phonon spectra of the two hosts needs to be considered. As the maximum-phonon energy and Debye temperature are considerably higher for $CdCl_2$, the Raman two-phonon process does not give any significant broadening until a temperature of about 50 K is reached (see broken lines in Fig. 6). At this temperature, one-phonon emission and absorption processes to levels at 30 cm^{-1} and 73 cm^{-1} away are significant as these levels are thermally populated by 50 K. At higher temperatures the Raman process prevails. In the case of $CdBr_2$, the Debye temperature is lower giving rapid line broadening from the Raman process above 30 K. Contributions of any one-phonon process between 40 and 70 K would be small compared to the onset of this broadening by the Raman process.

When comparing the $\bar{\alpha}$ values of the $\gamma_4^+ \rightarrow \gamma_{5,6}^+$ electronic transitions for $CdCl_2$ and $CdBr_2$, those for $CdBr_2$ are larger than for those $CdCl_2$ as expected for more covalent lattices. However, because of the presence of direct one-phonon process contributions, our results are not strong evidence for this dependence.

The electron-phonon coupling of Co^{2+} may be compared with the electron-phonon coupling found for the $^2E \rightarrow {}^4A_2$ spin-flip transition of Cr^{3+} in several oxide lattices and for $4f^n \rightarrow 4f^n$ transitions of the lanthanides. The $\bar{\alpha}$ values for the $^2E \rightarrow {}^4A_2$ emission of Cr^{3+} in $Y_3Al_5O_{12}$ (YAG) and $Y_3Ga_5O_{12}$ (YGG):Cr^{3+} are 233 and 685 cm^{-1} respectively.[8,9] The α values are 330 and 327 for YAG:Cr^{3+} and 419 and 450 cm^{-1} for YGG:Cr^{3+}.[8,9] For ruby and for MgO:Cr^{3+} $\bar{\alpha}$ values of about 600 cm^{-1} and 580 cm^{-1} were found.[10,11] These values of around 500 cm^{-1} are comparable to the 300 cm^{-1} found for $3d^7 \rightarrow 3d^7$ transitions for Co^{2+} and substantially larger than the 1 to 100 cm^{-1} determined for the lanthanides.[2]

C. $CdI_2:Co^{2+}$

For Co^{2+} in CdI_2 infrared-absorption spectra around 1000 cm^{-1} are yet to be reported and the positions of the spin-orbit and trigonal-crystal-field split components of the $^4T_{1g}$ term were established as part of this study. In Fig. 9 the infrared-absorption spectrum of CdI_2:1%Co^{2+} is shown. In analogy with Co^{2+} in $CdCl_2$ and $CdBr_2$, this spectrum shows three sharp absorption lines. One of these could be tentatively assigned as the electronic $\gamma_4^+ \rightarrow \gamma_{5,6}^+$ transition, while the other two are identified as vibronic lines associated

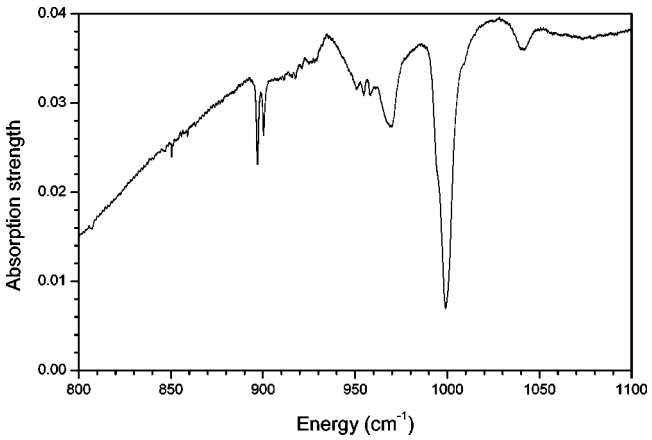

FIG. 9. 10 K infrared-absorption spectrum of CdI_2:1%Co^{2+}.

with the $\gamma_4^+ \rightarrow \gamma_4^+$ and $\gamma_4^+ \rightarrow \gamma_{5,6}^+$ transitions. The weak $\gamma_4^+ \rightarrow \gamma_4^+$ electronic transition was not observed.

Temperature-dependent line-broadening measurements performed on the three sharp-absorption lines of Co^{2+} in CdI_2 show a very rapid onset of broadening from low temperatures. The vibronic line at 897 cm^{-1} broadens from 1.1 cm^{-1} at 10 K to 4.5 cm^{-1} at 66 K. The vibronic line at 900.4 cm^{-1} broadens more rapidly from 1.2 cm^{-1} at 10 K to 8 cm^{-1} at 66 K. The weak line at 850.5 cm^{-1}, is only tentatively assigned and it was difficult to measure its broadening. From 10 to 20 K, this line broadened from 0.4 to 1.3 cm^{-1} and disappeared into the background at higher temperatures. Both the lower Debye temperature and the expected stronger electron-phonon interaction for the covalent CdI_2 lattice account for these rapid line-broadening changes with temperature.

V. CONCLUSIONS

The electron-phonon coupling for Co^{2+} $(3d^7)$ in three different cadmium halides has been investigated by measuring the line broadening and line shift of transitions between spin-orbit and trigonal-crystal-field levels of the $^4T_{1g}$ cubic-field ground term as a function of temperature. The line broadening of lines for Co^{2+} in $CdBr_2$ follow the behavior expected for Raman dephasing processes. For Co^{2+} in $CdCl_2$ contributions from direct one-phonon processes had to be included. Infrared transitions to levels of the $^4T_{1g}$ term for Co^{2+} in CdI_2 were measured and compared to those for Co^{2+} in $CdCl_2$ and $CdBr_2$.

ACKNOWLEDGMENT

The authors are grateful to Mr. Ross Ritchie for his help with growing the cobalt-doped cadmium halides.

[1] A. Meijerink, C. de Mello Donegá, A. Ellens, J. Sytsma, and G. Blasse, J. Lumin. **58**, 26 (1994).
[2] A. Meijerink, G. Blasse, J. Sytsma, C. de Mello Donegá, and A. Ellens, Acta Phys. Pol. A **90**, 109 (1996).
[3] A. Ellens, H. Andres, A. Meijerink, and G. Blasse, Phys. Rev. B **55**, 173 (1997).
[4] A. Ellens, H. Andres, M.L.H. ter Heerdt, R.T. Wegh, A. Meijerink, and G. Blasse, Phys. Rev. B **55**, 180 (1997).
[5] D.E. McCumber and M.D. Sturge, J. Appl. Phys. **34**, 1682 (1963).
[6] T. Kushida and M. Kikuchi, J. Phys. Soc. Jpn. **23**, 1333 (1967).
[7] G.F. Imbusch, W.M. Yen, D.E. McCumber, and M.D. Sturge, Phys. Rev. **133**, 1029 (1963).
[8] A.P. Vink and A. Meijerink, J. Lumin. **87-89**, 601 (2000).
[9] A.P. Vink and A. Meijerink, J. Phys. Chem. Solids **61**, 1717 (2000).
[10] A.P. Vink and A. Meijerink, Spectrochim. Acta, Part A **54**, 1755 (1998).
[11] A.P. Vink, M.A. de Bruin, and A. Meijerink, J. Phys.: Condens. Matter **12**, 8607 (2000).
[12] R.W.G Wyckoff, *Crystal Structures*, 2nd ed. (Wiley, New York, 1964), p. 270.
[13] R.E.M. Vickers, R.W.G. Syme, and D.J. Lockwood, J. Phys. C **18**, 2419 (1985).
[14] I.W. Johnstone and L. Dubicki, J. Phys. C **13**, 121 (1980).
[15] I.W. Johnstone and G.D. Jones, Phys. Rev. B **15**, 1297 (1977).
[16] J.C. Christie, I.W. Johnstone, G.D. Jones, and K. Zdansky, Phys. Rev. B **12**, 4656 (1975).
[17] G.F. Koster, J.O. Dimmock, R.G. Wheeler, and H. Statz, *Properties of the Thirty-Two Point Groups* (MIT Press, Cambridge, MA, 1963), p. 55.
[18] B. Henderson and G.F. Imbusch, *Optical Spectroscopy of Inorganic Solids* (Oxford University Press, London, 1989), p. 438.
[19] T. Hoshina, S. Imanaga, and S. Yokono, J. Lumin. **15**, 455 (1977).
[20] F. Auzel, G.F. de Sá, and W.M. de Azevedo, J. Lumin. **21**, 187 (1980).
[21] J.P.M. van Vliet and G. Blasse, J. Solid State Chem. **85**, 56 (1990).
[22] M. Galczyński and W. Stręk, J. Phys. Chem. Solids **52**, 681 (1991).
[23] M. Galczyński, M. Blażej, and W. Strek, Mater. Chem. Phys. **31**, 175 (1992).
[24] A. Meijerink, C. De Mello Donegá, A. Ellens, J. Sytsma, and G. Blasse, J. Lumin. **58**, 26 (1994).
[25] C. de Mello Donegá, A. Meijerink, and G. Blasse, J. Lumin. **62**, 189 (1994).